

MOL #81224

Solute restriction reveals an essential role for *clag3*-associated channels in malaria parasite nutrient acquisition

Ajay D. Pillai, Wang Nguitragool, Brian Lyko, Keithlee Dolinta, Michelle M. Butler, Son T. Nguyen, Norton P. Peet, Terry L. Bowlin, and Sanjay A. Desai

The Laboratory of Malaria and Vector Research, National Institute of Allergy and Infectious Diseases, National Institutes of Health, Bethesda, MD (ADP, WN, BL, KD, SAD); and Microbiotix, Inc., Worcester, MA (MMB, STN, NPP, TLB)

MOL #81224

Running Title Page

Running Title: *P. falciparum* requires channel-mediated nutrient uptake

Corresponding author: Sanjay A. Desai, M.D., Ph.D.

Laboratory of Malaria and Vector Research, National Institute of Allergy and Infectious Diseases, National Institutes of Health, 12735 Twinbrook Parkway, Room 3W-01
Rockville, MD 20852

Phone: 301-435-7552

E-mail: sdesai@niaid.nih.gov

Figures: 4

Tables: 2

Number of text pages: 20

References: 59

Word Count:

Abstract : 183

Introduction: 578

Discussion: 1,141

Non-standard Abbreviations: clag, cytoadherence linked antigen; hDHFR, human dihydrofolate reductase; ISPA, isolate-specific PSAC antagonist; PGIM, PSAC growth inhibition medium; PSAC, plasmodial surface anion channel; QTL, quantitative trait locus.

MOL #81224

Abstract

The plasmodial surface anion channel (PSAC) increases erythrocyte permeability to many solutes in malaria, but has uncertain physiological significance. We used a PSAC inhibitor with differing efficacies against channels from two *P. falciparum* parasite lines and found concordant effects on transport and *in vitro* parasite growth when external nutrient concentrations are reduced. Linkage analysis in a Dd2 x HB3 genetic cross using this growth inhibition phenotype mapped the *clag3* genomic locus, consistent with a role of two *clag3* genes in PSAC-mediated transport. Altered inhibitor efficacy, achieved via allelic exchange or expression switching between the *clag3* genes, indicates that this inhibitor kills parasites via direct action on PSAC. In a parasite unable to undergo expression switching, the inhibitor selected for ectopic homologous recombination between the *clag3* genes to increase the diversity of available channel isoforms. Broad spectrum inhibitors, which presumably interact with conserved sites on the channel, also had improved efficacy upon nutrient restriction. These findings indicate that PSAC functions in intracellular parasite nutrient acquisition. Although key questions about the channel and its biological role remain, antimalarial drug development targeting PSAC should be pursued.

MOL #81224

Introduction

Malaria parasites are successful single cell pathogens that cause immense morbidity and mortality in humans and other vertebrates. They have complex life cycles, but asexual replication within host erythrocytes is responsible for most clinical sequelae of malaria. *Plasmodium falciparum*, the most virulent human pathogen, remodels its host erythrocyte by exporting proteins (Boddey et al., 2010; Russo et al., 2010), generating membrane-bound organelles within the host cytosol (Tamez et al., 2008), and increasing erythrocyte permeability to numerous solutes (Ginsburg et al., 1983; Kirk et al., 1994).

The increased permeability is mediated by ion channels at the host erythrocyte membrane; it has been studied with tracer flux (Homewood and Neame, 1974; Saliba et al., 1998), osmotic fragility (Kutner et al., 1987), and patch-clamp techniques (Alkhalil et al., 2004; Staines et al., 2007; Alkhalil et al., 2012). Although several different channels have been proposed, recent studies with highly specific inhibitors support a single broad selectivity ion channel known as the plasmodial surface anion channel, PSAC (Pillai et al., 2010). PSAC has an unusually small single channel conductance for a broad selectivity channel (20 pS in 1.1 M Cl⁻) and is functionally conserved in divergent plasmodial species (Lisk and Desai, 2005). Two *clag3* genes from the parasite have been implicated in this channel activity through a molecular cloning strategy using an isolate-specific PSAC antagonist, ISPA-28, that blocks channels from only the Dd2 parasite line (Nguitragool et al., 2011).

Although direct evidence is missing, circumstantial observations suggest that PSAC activity is essential for intraerythrocytic parasite survival. First, both channel activity and the *clag* gene family are conserved in all plasmodial species examined to date (Lisk and Desai, 2005; Kaneko et al., 2001). Single channel patch-clamp studies have determined that even biophysical properties such as ion channel gating, conductance, and functional copy number/cell are nearly

MOL #81224

identical in *P. falciparum* and *P. knowlesi*, two divergent malaria parasites (Lisk and Desai, 2005). Second, gene silencing and mono-allelic expression of *clag3* genes in *P. falciparum* suggest that channel function is important (Cortes et al., 2007): parasites invest in expression switching for key gene families to evade host immunity and protect essential activities at the host cell surface (Scherf et al., 2008). Third, quantitative permeability studies for some required nutrients suggest that their PSAC-mediated uptake is needed for *in vitro* parasite cultivation (Gero and Wood, 1991; Saliba et al., 1998; Liu et al., 2006; Martin and Kirk, 2007). Finally, selections of parasite cultures with permeant toxins has generated functional PSAC mutants (Hill et al., 2007; Lisk et al., 2008), but has not yielded complete loss of function. These mutant channels exhibit reduced toxin uptake, but appear to satisfy the parasite's transport demands. Nevertheless, it remains possible that channel activity is a non-essential byproduct of host cell invasion (Staines et al., 2007). If the channel is required for parasite survival, the physiological role(s) it serves are debated, with proposals including nutrient uptake and metabolic waste removal (Desai et al., 2000), modification of host erythrocyte ionic composition (Brand et al., 2003), volume regulation of the infected cell (Staines et al., 2001; Lew et al., 2004), and autocrine purinergic signaling (Akkaya et al., 2009).

We have now addressed these uncertainties with functional and molecular studies using ISPA-28. This and other PSAC inhibitors exhibit improved efficacy in parasite growth inhibition studies when the concentrations of key nutrients are reduced. Genetic mapping, DNA transfection, and *in vitro* selections implicate the *clag3* genes in channel-mediated nutrient uptake required for parasite survival within erythrocytes.

MOL #81224

Materials and Methods

Parasite cultivation, design of PGIM, and growth inhibition studies. Asexual stage *P. falciparum* laboratory lines were propagated by standard methods in RPMI 1640 supplemented with 25 mM HEPES, 31 mM NaHCO₃, 0.37 mM hypoxanthine, 10 µg/mL gentamicin, and 10% pooled human serum. Nutrient deprivation experiments followed this standard medium, but used reduced concentrations of individual constituents; human serum was exhaustively dialyzed against distilled H₂O prior to addition to these media. PGIM contains reduced concentrations of isoleucine (11.4 µM), glutamine (102 µM), and hypoxanthine (3.01 µM) and was also supplemented with dialyzed serum.

Growth inhibition experiments were quantified using a SYBR Green I-based fluorescence assay for parasite nucleic acid in 96-well microplates, as described previously (Pillai et al., 2010). Ring-stage synchronized cultures were seeded at 1% parasitemia and 2% hematocrit in standard medium or PGIM and maintained for 72 h at 37 °C in 5% O₂, 5% CO₂ without media change. Cultures were then lysed in 20 mM Tris, 10 mM EDTA, 0.016% saponin, and 1.6% triton X100, pH 7.5 with SYBR Green I nucleic acid gel stain at a 5,000x dilution (Invitrogen, Carlsbad, CA). After a 45 min incubation, parasite DNA content was quantified by measuring fluorescence (excitation/emission wavelengths, 485/528 nm). For each inhibitor concentration, the mean of triplicate measurements was calculated after subtraction of background fluorescence from matched cultures killed by 20 µM chloroquine. Growth inhibition studies with the HB3^{3rec} parasite were performed after transport-based selection with ISPA-28 to achieve expression of the chimeric *clag3* gene generated by allelic exchange transfection. Limiting dilution culture to obtain parasite clones was performed in 96-well microplates with detection of positive wells by the C-SNARF method (Lyko et al., 2012).

MOL #81224

Parasites were also cultivated in pooled human serum collected from non-fasting donors (Interstate Blood Bank, Memphis, TN). The serum was ultracentrifuged (300,000 x g, 1h) to remove buoyant lipoproteins and used in 72 h cultivation experiments in microplates as above. Growth was quantified as above, except that microplate wells were washed once with PBS prior to addition of buffered SYBR Green I gel stain to eliminate serum-associated fluorescence artifacts.

Transport inhibition assays. Inhibitor affinity for PSAC block was determined using a quantitative transmittance assay based on osmotic lysis of infected cells in sorbitol (Pillai et al., 2010). Parasite cultures were enriched at the trophozoite stage using the percoll-sorbitol method, washed, and resuspended at 37 °C and 0.15% hematocrit in 280 mM sorbitol, 20 mM Na-HEPES, 0.1 mg/ml BSA, pH 7.4 with indicated inhibitor concentrations. Osmotic lysis due to PSAC-mediated sorbitol uptake was continuously tracked with transmittance measurements through the cell suspension (700 nm wavelength, DU640 spectrophotometer with Peltier temperature control, Beckman Coulter, Brea, CA). Inhibitor dose responses were calculated from the time required to reach a fractional lysis threshold. ISPA-28 dose responses were fitted to the sum of two Langmuir isotherms:

$$P = a / (1 + (x/b)) + (1-a) / (1 + (x/c)) \quad (\text{Eq. 1})$$

where P represents the normalized sorbitol permeability in the presence of inhibitor at concentration x , and a , b , and c are constants. Dose responses for other inhibitors were adequately fitted by a single Langmuir isotherm.

To examine possible inhibitor metabolism in parasite culture, we cultivated Dd2 parasites in standard media with 40 μ M ISPA-28 at 37 °C for 72 h. After centrifugation, the culture

MOL #81224

supernatant was used as a source of ISPA-28 for comparison to freshly prepared compound in transport inhibition studies.

QTL analysis. We sought genetic loci associated with ISPA-28 growth inhibitory efficacy in the Dd2 x HB3 genetic cross (Wellems et al., 1990) using 448 previously selected polymorphic markers that distinguish the Dd2 and HB3 parental lines (Nguitragool et al., 2011). QTL analysis was performed using R/qtl software (freely available at <http://www.rqtl.org/>) as described (Broman et al., 2003) and conditions suitable for the haploid asexual parasite. A $P = 0.5$ significance threshold was estimated with permutation analysis. Growth inhibition data at 0.3 and 10 μM ISPA-28 identified the same locus we report with 3 μM ISPA-28. Additional QTL were sought with secondary scans by controlling for the *clag3* locus.

Quantitative RT-PCR. Two-step real-time PCR was used to quantify *clag* gene expression using allele-specific primers developed previously (Nguitragool et al., 2011). RNA was harvested from schizont-stage cultures with TRIzol reagent (Invitrogen), treated with DNase, and used for reverse transcription (SuperScriptIII and oligo-dT priming, Invitrogen). Negative control reactions without reverse transcriptase confirmed there was no genomic DNA contamination. Real-time PCR was performed with QuantiTect SyBr Green PCR kit (Qiagen, Valencia, CA), the iCycler iQ multicolor real-time PCR system (Bio-Rad, Hercules, CA), and *clag* gene-specific primers (Supplemental Table 1). Serial dilution of parasite genomic DNA was used to construct the standard curve for each primer pair. PF7_0073 was used as a loading control as it is constitutively expressed. Transcript abundance for each *clag* gene was then determined from amplification kinetics.

MOL #81224

PCR studies for *clag3* recombination. The *clag3* locus of Dd2-*PGIM28* was characterized with genomic DNA and allele-specific primers: *3.1f* (5'-GTGCAATATATCAAAGTGACATGCA-3'), *3.1r* (5'-AAGAAAATAAATGCAAACAAGTTAGA-3'), *3.2f* (5'-GTTGAGTACGCACTAATATGTCAATTTG-3'), and *3.2r* (5'-AACCATAACATTATCATATATGTTAATTACAC-3'). cDNA prepared from schizont-stage cultures was also used with these primers to examine expression of both native and chimeric *clag3* genes.

Southern Blot. A *clag3*-specific probe was prepared by PCR amplification from Dd2 genomic DNA using 5'-ATTACAAACAAGAAGCTCAAGAGGA-3' and 5'-TTTTCTATATCTTCATTTCTTTAATTGTTTC-3' in the presence of Digoxigenin (DIG)-dUTP (Roche, Basel, Switzerland). Probe specificity was confirmed by blotting against full-length PCR amplicons of the five *clag* genes generated from Dd2 genomic DNA with primers listed in Supplemental Table 2.

Genomic DNA was digested with indicated restriction enzymes (New England BioLabs, Ipswich, MA), subjected to electrophoresis in 0.7% agarose, acid depurinated, transferred and crosslinked to Nylon membranes. The blot was then hybridized overnight at 39 °C with the above DIG-labeled probe in DIG Easy Hyb (Roche), and washed with low and high stringency buffers (2X SSC, 0.1% SDS, 23 °C followed by 1X SSC, 0.5% SDS, 50 °C) prior to DIG immunodetection according to the manufacturer's instructions.

Mammalian Cytotoxicity. Inhibitor cytotoxicity was quantified using human HeLa cells (ATCC# CLL-2) seeded at 4000 cells/well in 96-well plates. Cultures were incubated with individual inhibitors at 37°C for 72 h in Minimal Essential Medium (Gibco/Invitrogen)

MOL #81224

supplemented with 10% fetal calf serum. Cell viability was quantified using the vital stain MTS [3-(4,5-dimethylthiazol-2-yl)-5-(3-carboxymethoxyphenol)-2-(4-sulfophenyl)-2H-tetrazolium, inner salt], as described (Marshall et al., 1995). The reported CC_{50} value is the concentration of an inhibitor that reduces conversion of MTS to formazan by 50%.

Results

Poor growth inhibition by ISPA-28 under standard culture conditions. ISPA-28 blocks PSAC on Dd2-infected cells with high affinity and has only weak activity against channels from HB3 parasites ($K_{0.5}$ of 56 ± 5 nM and 43 ± 2 μ M, respectively; Nguitragool et al., 2011). If channel activity serves an essential role, this small molecule inhibitor should interfere with propagation of Dd2 cultures but spare those of HB3. Disappointingly, our initial *in vitro* parasite growth studies revealed an insignificant difference with both parasite lines exhibiting sustained growth in RPMI 1640-based media despite high ISPA-28 concentrations (IC_{50} values > 40 μ M for both lines, data not shown).

We considered possible explanations and determined that ISPA-28 efficacy against Dd2 channels is not compromised by metabolism of the inhibitor under *in vitro* culture conditions (Supplemental Fig. 1A). ISPA-28 is also not significantly adsorbed by serum protein or lipids, a phenomenon known to reduce activity of some PSAC inhibitors and many therapeutics (Supplemental Fig. 1B-D; Matsuhisa et al., 1987). Thus, ISPA-28 has unexpectedly poor efficacy against growth of Dd2 parasites.

One possibility is that channel activity is essential for malaria parasites, but that low level transport remaining in the presence of inhibitor adequately meets parasite demands under standard *in vitro* culture conditions. Consistent with this, we noticed sustained channel-mediated uptake in Dd2-infected erythrocytes even with high ISPA-28 concentrations; significantly less

MOL #81224

residual uptake was observed with compound **2**, a broad spectrum PSAC inhibitor with a comparable inhibitory $K_{0.5}$ value for Dd2 channels (Supplemental Fig. 2; $P < 10^{-4}$ for comparison of these inhibitors at 10 μM). The unexpected difference in residual channel activity with these inhibitors may account for their differing efficacies against *in vitro* parasite growth (IC_{50} values of $>40 \mu\text{M}$ and $4.7 \mu\text{M}$, respectively; Table 1).

Incomplete block with high ISPA-28 concentrations despite a low $K_{0.5}$ value for Dd2 channels suggests a complex mechanism of inhibition. While dantrolene and furosemide dose responses are adequately fitted by the equation that assumes a 1:1 stoichiometry for inhibitor and channel molecules (Langmuir isotherm; solid lines, Supplemental Fig. 1C and D), the ISPA-28 dose response was not well fit (Supplemental Fig. 2, blue dashed line). An improved fit was obtained with a two-component Langmuir equation (solid line). Because this two-component equation is compatible with several possible mechanisms, the ISPA-28 stoichiometry and precise mode of channel block remain unknown.

ISPA-28 inhibits growth of Dd2 but not of HB3 upon nutrient restriction. If PSAC functions in nutrient acquisition for the intracellular parasite (Desai et al., 2000), then the incomplete inhibition by ISPA-28 may permit adequate nutrient uptake. This effect may be accentuated under *in vitro* culture using RPMI 1640-based formulations, which contain high nutrient concentrations to support growth of diverse cell lines (Sato and Kan, 2001). The large inward concentration gradient for nutrients in such media may sustain parasite nutrient uptake despite near-complete channel block.

To evaluate this possibility, we examined parasite requirement for isoleucine, an essential amino acid that the parasite cannot synthesize *de novo* (Istvan et al., 2011). Isoleucine is absent from human hemoglobin, which the parasite digests as a source of some amino acids; it must be

MOL #81224

acquired by uptake from serum (Liu et al., 2006; Martin and Kirk, 2007). We prepared RPMI 1640 media with a range of isoleucine concentrations and determined that Dd2 and HB3 parasites have quantitatively similar isoleucine requirements, with negligible growth when this amino acid is removed from media (Fig. 1A, black symbols; EC_{50} values of 10-16 μ M isoleucine). Addition of 15 μ M ISPA-28 significantly increased Dd2 requirement for isoleucine (EC_{50} of $34.6 \pm 1.1 \mu$ M; $P < 10^{-9}$, Student's *t* test), but had no effect on HB3 parasites. This effect suggests an essential role for PSAC-mediated isoleucine uptake and is consistent with transport studies that show this channel is a major route of uptake after infection.

Because many nutritive solutes have significant PSAC permeability, we also examined parasite growth in RPMI-1640 media upon isolated removal of several other solutes: calcium panthothenate, cysteine, glutamic acid, glutamine, methionine, proline, and tyrosine. Hypoxanthine, a purine source not present in RPMI 1640 but commonly added to parasite culture media, was also evaluated. Each of these solutes has documented PSAC permeability (Ginsburg et al., 1985; Asahi et al., 1996; Gero and Wood, 1991; Saliba et al., 1998; Lisk et al., 2006), but some also exhibit uptake via host transporters on the erythrocyte membrane (Winterberg et al., 2012; Quashie et al., 2010). Microscopic examination of parasites propagated in these single depletion experiments revealed the greatest detriment upon removal of glutamine and hypoxanthine, but short-term growth studies revealed relatively modest effects (Fig. 1B-C). Addition of ISPA-28 did not measurably increase Dd2 requirement of either solute in these experiments.

Because parasite growth reflects a complex interplay of multiple biochemical pathways and the availability of nutrients that feed into them, the effects of PSAC inhibition may be greater than predicted from deprivation studies restricted to single solutes. We therefore simultaneously varied concentrations of isoleucine, glutamine, and hypoxanthine without manipulating other

MOL #81224

constituents in the RPMI 1640-based medium. This approach revealed conditions that increased ISPA-28 potency against Dd2 parasites while preserving the compound's negligible effect against HB3 (Fig. 2A).

In the absence of transport inhibitors, this medium, termed PSAC Growth Inhibition Medium (PGIM), permitted continuous propagation of both Dd2 and HB3 parasites (> 2 weeks), though at somewhat reduced rates (Fig. 2B, black bars). We noticed that cultures with low parasitemias grew well in PGIM but that rates decreased with higher parasite burden, consistent with nutrient limitation and competition amongst parasites in culture. To explore how these conditions may compare to *in vivo* expansion rates, we also examined parasite propagation in pooled, non-fasting serum collected from healthy donors. Human serum, when not subjected to dilution by synthetic media, also yielded relatively slow expansion of parasite cultures (Fig. 2B, white bars), consistent with the view that RPMI 1640-based formulations achieve high culture expansion rates through use of supraphysiological nutrient levels.

Linkage analysis and DNA transfection implicate *clag3* genes and PSAC inhibition.

Although the ISPA-28 growth IC_{50} values in PGIM ($0.66 \pm 0.20 \mu\text{M}$ and $52 \pm 19 \mu\text{M}$ for Dd2 and HB3, respectively; $P < 10^{-4}$) agree reasonably well with this inhibitor's transport $K_{0.5}$ values, differing efficacies against parasite growth might also reflect the inhibitor's effects on other parasite targets. We therefore examined the ISPA-28 growth inhibition phenotype in the progeny of the Dd2 x HB3 genetic cross (Wellems et al., 1990). These studies revealed a broad range of ISPA-28 efficacies for progeny clones (Fig. 2C), with many progeny resembling one or the other parent. Because HB3 and some progeny had high growth IC_{50} values that could not be precisely estimated, linkage analysis was performed using growth inhibition at $3 \mu\text{M}$ ISPA-28, a concentration that optimally distinguishes the parental phenotypes. This analysis identified a

MOL #81224

single parasite genomic locus at the 5' end of chromosome 3 with high confidence (Fig. 2D, LOD score of 12.7). Additional contributing genomic loci were sought by removing the effects of this locus, but were not identified in secondary scans (Supplemental Fig. 3).

The mapped locus contains many genes but most notably the two *clag3* genes recently implicated in PSAC activity. To determine if the proteins encoded by these genes are the growth inhibitory targets of ISPA-28, we performed studies with HB3^{3rec}, a parasite clone generated by allelic exchange transfection of HB3 to replace the 3' end of the native *clag3.2* gene with the corresponding fragment from the *clag3.1* of Dd2. When this chimeric gene is expressed, HB3^{3rec} exhibits high affinity inhibition by ISPA-28 ($K_{0.5}$ of 51 ± 9 nM, $P = 0.88$ for no difference from Dd2; Nguitragool et al., 2011). In PGIM-based growth inhibition studies, HB3^{3rec} was highly sensitive to ISPA-28 at levels that matched Dd2 parasites (Fig. 2E), indicating that ISPA-28 toxicity is mediated through action on the *clag3* product. Moreover, the requirement for nutrient restriction to detect this compound's growth inhibitory effect supports a primary role of PSAC in parasite nutrient acquisition.

Selective growth of parasites with resistant *clag3* alleles. We explored the channel's role further by evaluating whether PSAC inhibitors and PGIM can be used to selectively kill parasites that express individual *clag3* genes. Most laboratory parasite lines carry two *clag3* genes on chromosome 3, but individual parasites appear to express only one allele at a time (Fig. 3A). Silencing of the other allele is thought to occur via epigenetic mechanisms (Cortes et al., 2007). This process, along with relatively slow rates of switching between the two alleles, allows subsets of parasites to escape host immune responses against surface-exposed antigens.

ISPA-28 specifically inhibits channels associated with the Dd2 *clag3.1* gene because it binds to a region near the C-terminus of the encoded protein; it has little or no activity against channels

MOL #81224

linked to expression of Dd2 *clag3.2* or of either *clag3* in unrelated parasite lines (Nguiragool et al., 2011). This inhibitor has previously been used to select for Dd2 *clag3.1* expression through osmotic lysis of infected cells in sorbitol, a sugar alcohol with high PSAC permeability. Sorbitol solutions containing ISPA-28 select for this allele because osmotic lysis eliminates infected cells whose channels are not blocked (Fig. 3B, transport selection).

Here, we hypothesized that ISPA-28 and PGIM may be useful in counter-selections for other *clag3* alleles (Fig. 3B, PGIM growth selection). While sorbitol-induced osmotic lysis selects for expression of the ISPA-28 sensitive *clag3.1*, growth inhibition in PGIM should favor cells expressing the resistant *clag3.2* allele because only parasites expressing unblocked channels should meet their nutrient demands and propagate successfully. We first examined the progeny clone 7C20, which carries the Dd2 *clag3* locus and expresses both alleles in unselected cultures (Figs. 3C-E). After selection with osmotic lysis in sorbitol and ISPA-28, surviving parasites had PSAC inhibitor affinity matching the Dd2 parent and predominantly expressed the *clag3.1* allele. The culture was then propagated in PGIM containing 5 μ M ISPA-28 for a total of 10 days; microscopic examination of smears during this treatment revealed near complete sterilization of the culture. Channels expressed by parasites that survived this second treatment had markedly reduced ISPA-28 affinity, indicating that *in vitro* propagation with PSAC inhibitors can be used to select for rare parasite subpopulations. Consistent with our predictions, RT-PCR confirmed strong negative selection against *clag3.1* to yield parasites that preferentially express *clag3.2*. There were also modest changes in expression of *clag* genes on other chromosomes, suggesting that these paralogs may also contribute to PSAC activity. Importantly, the opposing effects of ISPA-28 on *in vitro* growth inhibition and on susceptibility to transport-induced osmotic lysis permit purifying selections of either *clag3* allele and reveal a strict correlation with channel phenotype.

MOL #81224

Genomic recombination to overcome a defect in epigenetic switching. Surprisingly, the Dd2 parental line retains exclusive expression of *clag3.1* in unselected cultures despite being isogenic with 7C20 at the *clag3* locus. To explore possible mechanisms, we sought to select for Dd2 parasites expressing the alternate *clag3.2* allele. We first tried transport selection using osmotic lysis with ISPA-43 (Supplemental Fig. 4A), an unrelated PSAC inhibitor with higher affinity for channels formed by expression of the Dd2 *clag3.2* than of *clag3.1*. Although this approach has been successfully used to select for 7C20 parasites expressing *clag3.2* (Nguitragool et al., 2011), it proved insufficient to affect channel phenotype in Dd2 parasites despite repeated selections over 4 months (Supplemental Figs. 4B-C).

We next attempted negative selection with growth inhibition in PGIM containing ISPA-28. After 2 cycles of drug pressure with 5 μ M ISPA-28 for a total of 17 days, resistant cells were identified and characterized after limiting dilution to obtain the clone Dd2-PGIM28. Consistent with killing primarily via PSAC inhibition, transport studies using this resistant clone revealed a marked reduction in inhibitor affinity (Fig. 4A). Surprisingly, although the ISPA-28 dose response quantitatively matched that of 7C20 parasites after identical PGIM-based selection (upper solid line, Fig. 4A), full length *clag3.2* transcript was still undetectable (Fig. 4B). Because this observation excludes simple gene switching, we considered spontaneous recombination between the two *clag3* genes. We identified a chimeric *clag3* transcript using a forward *clag3.1* primer and a reverse *clag3.2* primer; PCR confirmed that this chimera is present in the selected parasite's genome but absent from the original Dd2 line (Fig. 4C). Southern blotting with a *clag3* specific probe detected three discrete bands in the selected clone but only the expected two bands in unselected Dd2 parasites (Fig. 4D; Supplemental Fig. 5 showing probe specificity), implicating a recombination event to produce three *clag3* genes in Dd2-PGIM28

MOL #81224

(Fig. 4E). The size of the new band, ~ 16 kb, matches the intergenic distance between *clag3.1* and *clag3.2* and is consistent with homologous recombination in Dd2-*PGIM28*. DNA sequencing indicated that the chimeric gene derives its 5' untranslated region and the first ~70% of the gene from *clag3.1*. After a crossover between single nucleotide polymorphisms at 3680 and 3965 bp from the start codon, the gene carries the 3' end of *clag3.2*. Thus, the chimeric gene is driven by the *clag3.1* promoter, but encodes a protein with the C-terminal variable domain of *clag3.2*. This altered C-terminus accounts for the reduced ISPA-28 efficacy against nutrient uptake and, hence, survival of this clone in our selection. Such homologous recombination also produces a parasite having a single *clag3* gene and high ISPA-28 affinity, but that recombinant is not expected to survive growth inhibition selection in PGIM with ISPA-28.

We used quantitative RT-PCR to examine transcription of *clag* genes in Dd2-*PGIM28* and found that the chimeric gene is preferentially expressed (Fig. 4F; 8.9 ± 1.3 fold greater than *clag3.1*, $P < 0.002$). We then performed transport-based selection with sorbitol and ISPA-28 to examine whether Dd2-*PGIM28* can undergo expression switching. As expected for an intact *clag3.1* promoter and gene, this second selection yielded parasites that express the native *clag3.1* almost exclusively (*PGIM-rev*, Figs. 4F-G). Transport studies revealed an ISPA-28 dose response identical to that of the original Dd2 line (Fig. 4H). Thus, the new chimeric *clag3* gene can undergo epigenetic silencing and switching with *clag3.1*. It is not clear why the native *clag3.2* gene of Dd2 parasites is refractory to transcription: DNA sequencing of the gene's promoter region did not reveal any mutations relative to that of 7C20.

Thus, recombination between the two *clag3* genes occurs with relative ease, consistent with reports of frequent recombination events in the parasite's subtelomeric regions (Freitas-Junior et al., 2000). Such recombination events may serve to increase diversity in PSAC phenotypes, apparent here as affording survival of a parasite with three *clag3* genes under selective pressure.

MOL #81224

Conserved PSAC inhibitors and antimalarial drugs that act at other targets. To further examine PSAC's physiological role, we next compared growth inhibitory effects of other PSAC inhibitors in PGIM and standard media (Table 1). Furosemide and dantrolene are known non-specific inhibitors with relatively low PSAC affinity. These compounds are also adsorbed by serum (Supplemental Fig. 1C-D), but are approved therapeutics in other human diseases. They are only weakly effective against parasite growth in standard medium, but have significantly improved activity in PGIM. We also tested 8 high affinity PSAC inhibitors from 5 distinct scaffolds recently identified by high-throughput screening (Pillai et al., 2010). Each of these inhibitors was also more potent when nutrient concentrations were reduced, strengthening the evidence for the channel's role in nutrient acquisition. The extent of improved efficacy was variable, but many compounds exhibited a >100-fold improvement in efficacy upon nutrient restriction (IC_{50} ratio, Table 1). Factors such as the stoichiometry of inhibitor:channel interaction and resultant changes in the concentration dependence of channel block (Supplemental Fig. 2), compound stability in culture, and adsorption by serum may influence the magnitude of this ratio for individual compounds.

To explore therapeutic potential, we then examined *in vitro* HeLa cell cytotoxicity. Several potent PSAC inhibitors were found to be nontoxic (Table 2), suggesting that they may be excellent starting points for medicinal chemistry optimization to develop new antimalarial drugs that target parasite nutrient uptake.

Finally, we performed *in vitro* growth inhibition experiments with chloroquine, mefloquine, and artemisinin, approved antimalarial drugs that work at unrelated targets within the intracellular parasite. Each of these drugs was modestly less active in PGIM than in standard medium (Table 1), providing evidence against nonspecific effects of modified *in vitro* growth

MOL #81224

conditions. The improved efficacy of PSAC inhibitors upon nutrient restriction is in contrast to the effect on existing antimalarial drugs and, therefore, implicates a distinct mechanism of action.

Discussion

Conservation of both PSAC activity and the recently implicated *clag3* genes in rodent, avian, and primate malaria species suggests that this ion channel serves an important role for the intracellular parasite. Because the channel is absent from other apicomplexan parasites and higher organisms (Alkhalil et al., 2007), inhibitors may be suitable starting points for development of highly specific antimalarial drugs. However, PSAC's biological role was unclear; concerns that the channel might be only an epiphenomenon of infection hampered progress toward therapeutics (Staines et al., 2007). Here, we addressed this uncertainty with isolate-specific and broad spectrum PSAC inhibitors, linkage analysis in a genetic cross, molecular studies, and *in vitro* selections. These studies provide experimental evidence for an essential and targetable role of PSAC in nutrient acquisition for the intracellular parasite.

Previous growth inhibition studies with PSAC inhibitors have consistently reported discrepancies between the concentrations required for transport inhibition and those needed to inhibit *in vitro* parasite growth (Pillai et al., 2010; Staines et al., 2004). In light of our findings, this discrepancy likely results from use of RPMI formulations, which were designed with high concentrations of many nutrients to maximize growth of diverse cell types. Our examination of individual substrates revealed that isoleucine uptake via PSAC serves an essential role for the parasite. Plasma isoleucine concentrations in developed countries range between 60 and 95 μM (Armstrong and Stave, 1973; Milsom et al., 1979), with values in malarious countries likely to be lower (Saunders et al., 1967). These measured values are not only significantly lower than the

MOL #81224

381 μM in RPMI 1640, but they fall into a range where dose response studies suggest that PSAC-mediated uptake is rate-limiting (Fig. 1A). Although glutamine and hypoxanthine dose response studies did not show similar effects on their own, their combined restriction to produce PGIM yielded further improvements in PSAC inhibitor efficacy. Future refinements of PGIM to include other permeant nutrients having high concentrations in RPMI 1640 may yield additionally improved *in vitro* PSAC inhibitor efficacy. Separate studies, such as *in vivo* efficacy studies in rodent malaria models, will be necessary to determine whether our findings can be translated into future antimalarial drugs.

Marked changes in inhibitor efficacy after relatively modest manipulations raise questions about the optimal conditions for high-throughput screens that use *in vitro* growth inhibition to find antimalarial drug leads; to date, these screens have used only the standard RPMI 1640 medium (Plouffe et al., 2008; Gamo et al., 2010; Guiguemde et al., 2010). Although three existing antimalarial drugs had unchanged efficacy upon nutrient restriction (Table 1), it is important to recognize that *in vitro* parasite growth depends on many factors. We envision that compounds acting at some downstream sites involved in nutrient utilization or metabolism will also exhibit improved efficacy in more physiological media such as PGIM. Such compounds may act synergistically with PSAC inhibitors. Future high-throughput screens that quantify parasite growth inhibition should consider the medium and other growth conditions carefully; conditions that most closely reproduce *in vivo* parasite development may be fruitful.

While our studies provide additional evidence for the involvement of parasite *clag3* genes in PSAC activity, there are still fundamental questions about the composition and structure of this unusual ion channel (Desai, 2012). Prior studies of these genes are also largely consistent with our findings (Cortes et al., 2007; Vincensini et al., 2008; Kaneko et al., 2001), but there are some interesting discrepancies with a reported *clag3* knockdown parasite (Comeaux et al., 2011). That

MOL #81224

study used DNA transfection to disrupt *clag3.2* and replace it with the hDHFR selectable marker; subsequent application of WR99210 led to expression of hDHFR and silencing of *clag3.1*, presumably through the epigenetic mechanisms characterized here. Because both native *clag3* genes had undetectable expression in their study, their findings contrast with the essential role in nutrient uptake proposed here. PSAC activity remains to be examined in the knockdown parasite; molecular studies are also required to explore ectopic recombination or other compensatory changes that circumvent gene suppression (Fig. 4). Another possibility, that only some parasite lines require channel-mediated nutrient uptake, may reconcile our findings with a viable *clag3* knockdown parasite. In this case, surveys of clinical isolates from malaria patients may reveal novel PSAC-null parasite lines. Such studies should be pursued as they are complementary to *in vivo* efficacy studies in rodent malaria species.

Allele-specific inhibitors, such as ISPA-28, represent useful reagents for examining epigenetic silencing mechanisms. In addition to the *clag3* genes, several other parasite gene families exhibit regulated expression and switching to increase antigenic diversity and achieve immune evasion (Scherf et al., 1998; Mok et al., 2007; Lavazec et al., 2007; Deitsch et al., 2009). ISPA-28 is especially useful because it can be used in both positive and negative selections for the Dd2 *clag3.1* gene: our transport and growth inhibition strategies permit selection of channels that are either sensitive or resistant to this inhibitor. By combining these strategies, we identified a defect in *clag3* gene switching in the Dd2 line; intact switching in the 7C20 parasite, which is isogenic at the chromosome 3 locus, excludes defects in cis-regulatory elements such as the promoter and instead suggests other determinants, possibly transcription factors (Tonkin et al., 2009). Our selections also show that Dd2 parasites can overcome this switching defect by ectopic recombination between the two *clag3* genes to produce a new chimeric gene. This chimeric gene is transcription-competent and encodes ISPA-28 resistant channels. Similar

MOL #81224

recombination events have been documented for other virulence genes within subtelomeric regions of the parasite genome (Kraemer and Smith, 2003); they likely account for the observed variation in *clag3* copy number of common laboratory parasite lines (Chung et al., 2007).

Our studies suggest that nutrient uptake at the host membrane is rate-limiting. Although our understanding of PSAC composition and precise *in vivo* role remains limited, our findings support continued pursuit of antimalarial drug discovery targeting this unusual ion channel. This target is especially attractive because some available PSAC inhibitors sterilize cultures at clinically achievable concentrations, with efficacies comparable to those of existing antimalarial drugs (PGIM IC_{50} values, Table 1). A legitimate concern relates to functional differences between channels of distinct parasite lines and associated polymorphisms in the *clag3* product (Alkhalil et al., 2004; Alkhalil et al., 2009; Nguitragool et al., 2011). Will such variability reduce clinical effectiveness against malaria or speed drug resistance? We do not think so. Critical channel properties, such as the list of permeant solutes and their relative transport rates, are strictly conserved in *P. falciparum* and other malaria parasite species (Lisk and Desai, 2005). Paralleling this observation, informatic analyses of the *clag3* product reveal highly conserved domains separated by only a few polymorphic regions. In addition to sites that function in solute recognition and permeation, domains that function in trafficking, insertion, and regulation of the channel at the host erythrocyte surface may also be conserved and, therefore, targetable.

MOL #81224

Acknowledgments

We dedicate this manuscript to the memory of Ian Bathurst, the Medicines for Malaria Venture Project Director for these studies.

Author Contributions

Participated in research design: Pillai, Nguitragool, Lyko, Dolinta, Butler, Nguyen, Peet, Bowlin, and Desai.

Conducted experiments: Pillai, Nguitragool, Lyko, Dolinta, Butler, Nguyen, and Desai.

Performed data analysis: Pillai, Nguitragool, Lyko, Dolinta, Butler, Nguyen, Peet, Bowlin, and Desai.

Wrote or contributed to the writing of the manuscript: Pillai, Nguitragool, Lyko, Dolinta, Butler, Nguyen, Peet, Bowlin, and Desai.

MOL #81224

References

- Akkaya C, Shumilina E, Bobballa D, Brand VB, Mahmud H, Lang F and Huber SM (2009) The *Plasmodium falciparum*-induced anion channel of human erythrocytes is an ATP-release pathway. *Pflugers Arch* **457**:1035-1047.
- Alkhalil A, Cohn JV, Wagner MA, Cabrera JS, Rajapandi T and Desai SA (2004) *Plasmodium falciparum* likely encodes the principal anion channel on infected human erythrocytes. *Blood* **104**:4279-4286.
- Alkhalil A, Hill DA and Desai SA (2007) Babesia and plasmodia increase host erythrocyte permeability through distinct mechanisms. *Cell Microbiol* **9**:851-860.
- Alkhalil A, Hong L, Nguitragool W and Desai SA (2012) Voltage-dependent inactivation of the plasmodial surface anion channel via a cleavable cytoplasmic component. *Biochim Biophys Acta* **1818**:367-374.
- Alkhalil A, Pillai AD, Bokhari AA, Vaidya AB and Desai SA (2009) Complex inheritance of the plasmodial surface anion channel in a *Plasmodium falciparum* genetic cross. *Mol Microbiol* **72**:459-469.
- Armstrong MD and Stave U (1973) A study of plasma free amino acid levels. II. Normal values for children and adults. *Metabolism* **22**:561-569.
- Asahi H, Kanazawa T, Kajihara Y, Takahashi K and Takahashi T (1996) Hypoxanthine: a low molecular weight factor essential for growth of erythrocytic *Plasmodium falciparum* in a serum-free medium. *Parasitology* **113** (Pt 1):19-23.
- Boddey JA, Hodder AN, Gunther S, Gilson PR, Patsiouras H, Kapp EA, Pearce JA, de Koning-Ward TF, Simpson RJ, Crabb BS and Cowman AF (2010) An aspartyl protease directs malaria effector proteins to the host cell. *Nature* **463**:627-631.
- Brand VB, Sandu CD, Duranton C, Tanneur V, Lang KS, Huber SM and Lang F (2003) Dependence of *Plasmodium falciparum* *in vitro* growth on the cation permeability of the human host erythrocyte. *Cell Physiol Biochem* **13**:347-356.
- Broman KW, Wu H, Sen S and Churchill GA (2003) R/qtl: QTL mapping in experimental crosses. *Bioinformatics* **19**:889-890.
- Chung WY, Gardiner DL, Anderson KA, Hyland CA, Kemp DJ and Trenholme KR (2007) The CLAG/RhopH1 locus on chromosome 3 of *Plasmodium falciparum*: two genes or two alleles of the same gene? *Mol Biochem Parasitol* **151**:229-232.
- Comeaux CA, Coleman BI, Bei AK, Whitehurst N and Duraisingh MT (2011) Functional analysis of epigenetic regulation of tandem RhopH1/clag genes reveals a role in *Plasmodium falciparum* growth. *Mol Microbiol* **80**:378-390.
- Cortes A, Carret C, Kaneko O, Yim Lim BY, Ivens A and Holder AA (2007) Epigenetic silencing of *Plasmodium falciparum* genes linked to erythrocyte invasion. *PLoS Pathog* **3**:e107.

MOL #81224

Deitsch KW, Lukehart SA and Stringer JR (2009) Common strategies for antigenic variation by bacterial, fungal and protozoan pathogens. *Nat Rev Microbiol* **7**:493-503.

Desai SA (2012) Ion and nutrient uptake by malaria parasite-infected erythrocytes. *Cell Microbiol* **14**:1003-1009.

Desai SA, Bezrukov SM and Zimmerberg J (2000) A voltage-dependent channel involved in nutrient uptake by red blood cells infected with the malaria parasite. *Nature* **406**:1001-1005.

Freitas-Junior LH, Bottius E, Pirrit LA, Deitsch KW, Scheidig C, Guinet F, Nehrbass U, Welles TE and Scherf A (2000) Frequent ectopic recombination of virulence factor genes in telomeric chromosome clusters of *P. falciparum*. *Nature* **407**:1018-1022.

Gamo FJ, Sanz LM, Vidal J, de CC, Alvarez E, Lavandera JL, Vanderwall DE, Green DV, Kumar V, Hasan S, Brown JR, Peishoff CE, Cardon LR and Garcia-Bustos JF (2010) Thousands of chemical starting points for antimalarial lead identification. *Nature* **465**:305-310.

Gero AM and Wood AM (1991) New nucleoside transport pathways induced in the host erythrocyte membrane of malaria and Babesia infected cells. *Adv Exp Med Biol* **309A**:169-172.

Ginsburg H, Krugliak M, Eidelman O and Cabantchik ZI (1983) New permeability pathways induced in membranes of *Plasmodium falciparum* infected erythrocytes. *Mol Biochem Parasitol* **8**:177-190.

Ginsburg H, Kutner S, Krugliak M and Cabantchik ZI (1985) Characterization of permeation pathways appearing in the host membrane of *Plasmodium falciparum* infected red blood cells. *Mol Biochem Parasitol* **14**:313-322.

Guiguemde WA, Shelat AA, Bouck D, Duffy S, Crowther GJ, Davis PH, Smithson DC, Connelly M, Clark J, Zhu F, Jimenez-Diaz MB, Martinez MS, Wilson EB, Tripathi AK, Gut J, Sharlow ER, Bathurst I, El MF, Fowble JW, Forquer I, McGinley PL, Castro S, ngulo-Barturen I, Ferrer S, Rosenthal PJ, DeRisi JL, Sullivan DJ, Lazo JS, Roos DS, Riscoe MK, Phillips MA, Rathod PK, Van Voorhis WC, Avery VM and Guy RK (2010) Chemical genetics of *Plasmodium falciparum*. *Nature* **465**:311-315.

Hill DA, Pillai AD, Nawaz F, Hayton K, Doan L, Lisk G and Desai SA (2007) A blasticidin S-resistant *Plasmodium falciparum* mutant with a defective plasmodial surface anion channel. *Proc Natl Acad Sci USA* **104**:1063-1068.

Homewood CA and Neame KD (1974) Malaria and the permeability of the host erythrocyte. *Nature* **252**:718-719.

Istvan ES, Dharia NV, Bopp SE, Gluzman I, Winzeler EA and Goldberg DE (2011) Validation of isoleucine utilization targets in *Plasmodium falciparum*. *Proc Natl Acad Sci USA* **108**:1627-1632.

Kaneko O, Tsuboi T, Ling IT, Howell S, Shirano M, Tachibana M, Cao YM, Holder AA and Torii M (2001) The high molecular mass rhoptry protein, RhopH1, is encoded by members of

MOL #81224

the clag multigene family in *Plasmodium falciparum* and *Plasmodium yoelii*. *Mol Biochem Parasitol* **118**:223-231.

Kirk K, Horner HA, Elford BC, Ellory JC and Newbold CI (1994) Transport of diverse substrates into malaria-infected erythrocytes via a pathway showing functional characteristics of a chloride channel. *J Biol Chem* **269**:3339-3347.

Kraemer SM and Smith JD (2003) Evidence for the importance of genetic structuring to the structural and functional specialization of the *Plasmodium falciparum* var gene family. *Mol Microbiol* **50**:1527-1538.

Kutner S, Breuer WV, Ginsburg H and Cabantchik ZI (1987) On the mode of action of phlorizin as an antimalarial agent in *in vitro* cultures of *Plasmodium falciparum*. *Biochem Pharmacol* **36**:123-129.

Lavazec C, Sanyal S and Templeton TJ (2007) Expression switching in the stevor and Pfmc-2TM superfamilies in *Plasmodium falciparum*. *Mol Microbiol* **64**:1621-1634.

Lew VL, Macdonald L, Ginsburg H, Krugliak M and Tiffert T (2004) Excess haemoglobin digestion by malaria parasites: a strategy to prevent premature host cell lysis. *Blood Cells Mol Dis* **32**:353-359.

Lisk G and Desai SA (2005) The plasmodial surface anion channel is functionally conserved in divergent malaria parasites. *Eukaryot Cell* **4**:2153-2159.

Lisk G, Kang M, Cohn JV and Desai SA (2006) Specific inhibition of the plasmodial surface anion channel by dantrolene. *Eukaryot Cell* **5**:1882-1893.

Lisk G, Pain M, Gluzman IY, Kambhampati S, Furuya T, Su XZ, Fay MP, Goldberg DE and Desai SA (2008) Changes in the plasmodial surface anion channel reduce leupeptin uptake and can confer drug resistance in *P. falciparum*-infected erythrocytes. *Antimicrob Agents Chemother* **52**:2346-2354.

Liu J, Istvan ES, Gluzman IY, Gross J and Goldberg DE (2006) *Plasmodium falciparum* ensures its amino acid supply with multiple acquisition pathways and redundant proteolytic enzyme systems. *Proc Natl Acad Sci USA* **103**:8840-8845.

Lyko B, Hammershaimb EA, Nguitragool W, Wellem TE and Desai SA (2012) A high-throughput method to detect *Plasmodium falciparum* clones in limiting dilution microplates. *Malar J* **11**:124.

Marshall NJ, Goodwin CJ and Holt SJ (1995) A critical assessment of the use of microculture tetrazolium assays to measure cell growth and function. *Growth Regul* **5**:69-84.

Martin RE and Kirk K (2007) Transport of the essential nutrient isoleucine in human erythrocytes infected with the malaria parasite *Plasmodium falciparum*. *Blood* **109**:2217-2224.

Matsuhisa S, Takesawa S and Sakai K (1987) Binary-Solute Adsorption of Dosed Drugs on Serum-Albumin. *Chem Engineering J and the Biochemical Engineering J* **34**:B21-B27.

MOL #81224

Milsom JP, Morgan MY and Sherlock S (1979) Factors affecting plasma amino acid concentrations in control subjects. *Metabolism* **28**:313-319.

Mok BW, Ribacke U, Winter G, Yip BH, Tan CS, Fernandez V, Chen Q, Nilsson P and Wahlgren M (2007) Comparative transcriptomal analysis of isogenic *Plasmodium falciparum* clones of distinct antigenic and adhesive phenotypes. *Mol Biochem Parasitol* **151**:184-192.

Nguitragool W, Bokhari AA, Pillai AD, Rayavara K, Sharma P, Turpin B, Aravind L and Desai SA (2011) Malaria parasite clag3 genes determine channel-mediated nutrient uptake by infected red blood cells. *Cell* **145**:665-677.

Pillai AD, Pain M, Solomon T, Bokhari AA and Desai SA (2010) A cell-based high-throughput screen validates the plasmodial surface anion channel as an antimalarial target. *Mol Pharmacol* **77**:724-733.

Plouffe D, Brinker A, McNamara C, Henson K, Kato N, Kuhen K, Nagle A, Adrian F, Matzen JT, Anderson P, Nam TG, Gray NS, Chatterjee A, Janes J, Yan SF, Trager R, Caldwell JS, Schultz PG, Zhou Y and Winzeler EA (2008) In silico activity profiling reveals the mechanism of action of antimalarials discovered in a high-throughput screen. *Proc Natl Acad Sci USA* **105**:9059-9064.

Quashie NB, Ranford-Cartwright LC and De Koning HP (2010) Uptake of purines in *Plasmodium falciparum*-infected human erythrocytes is mostly mediated by the human equilibrative nucleoside transporter and the human facilitative nucleobase transporter. *Malar J* **9**:36.

Russo I, Babbitt S, Muralidharan V, Butler T, Oksman A and Goldberg DE (2010) Plasmepsin V licenses *Plasmodium* proteins for export into the host erythrocyte. *Nature* **463**:632-636.

Saliba KJ, Horner HA and Kirk K (1998) Transport and metabolism of the essential vitamin pantothenic acid in human erythrocytes infected with the malaria parasite *Plasmodium falciparum*. *J Biol Chem* **273**:10190-10195.

Sato JD and Kan M (2001) Media for culture of mammalian cells. *Curr Protoc Cell Biol* Chapter 1, Unit 1.2.

Saunders SJ, Truswell AS, Barbezat GO, Wittman W and Hansen JD (1967) Plasma free amino acid pattern in protein-calorie malnutrition. Reappraisal of its diagnostic value. *Lancet* **2**:795-797.

Scherf A, Hernandez-Rivas R, Buffet P, Bottius E, Benatar C, Pouvelle B, Gysin J and Lanzer M (1998) Antigenic variation in malaria: in situ switching, relaxed and mutually exclusive transcription of var genes during intra-erythrocytic development in *Plasmodium falciparum*. *EMBO J* **17**:5418-5426.

Scherf A, Lopez-Rubio JJ and Riviere L (2008) Antigenic variation in *Plasmodium falciparum*. *Annu Rev Microbiol* **62**:445-470.

MOL #81224

Staines HM, Alkhalil A, Allen RJ, De Jonge HR, Derbyshire E, Egee S, Ginsburg H, Hill DA, Huber SM, Kirk K, Lang F, Lisk G, Oteng E, Pillai AD, Rayavara K, Rouhani S, Saliba KJ, Shen C, Solomon T, Thomas SL, Verloo P and Desai SA (2007) Electrophysiological studies of malaria parasite-infected erythrocytes: current status. *Int J Parasitol* **37**:475-482.

Staines HM, Dee BC, O'Brien M, Lang HJ, Englert H, Horner HA, Ellory JC and Kirk K (2004) Furosemide analogues as potent inhibitors of the new permeability pathways of *Plasmodium falciparum*-infected human erythrocytes. *Mol Biochem Parasitol* **133**:315-318.

Staines HM, Ellory JC and Kirk K (2001) Perturbation of the pump-leak balance for Na⁺ and K⁺ in malaria- infected erythrocytes. *Am J Physiol Cell Physiol* **280**:C1576-C1587.

Tamez PA, Bhattacharjee S, van OC, Hiller NL, Llinas M, Balu B, Adams JH and Haldar K (2008) An erythrocyte vesicle protein exported by the malaria parasite promotes tubovesicular lipid import from the host cell surface. *PLoS Pathog* **4**:e1000118.

Tonkin CJ, Carret CK, Duraisingh MT, Voss TS, Ralph SA, Hommel M, Duffy MF, Silva LM, Scherf A, Ivens A, Speed TP, Beeson JG and Cowman AF (2009) Sir2 paralogue cooperate to regulate virulence genes and antigenic variation in *Plasmodium falciparum*. *PLoS Biol* **7**:e84.

Vincensini L, Fall G, Berry L, Blisnick T and Braun BC (2008) The RhopH complex is transferred to the host cell cytoplasm following red blood cell invasion by *Plasmodium falciparum*. *Mol Biochem Parasitol* **160**:81-89.

Wellems TE, Panton LJ, Gluzman IY, do Rosario VE, Gwadz RW, Walker-Jonah A and Krogstad DJ (1990) Chloroquine resistance not linked to mdr-like genes in a *Plasmodium falciparum* cross. *Nature* **345**:253-255.

Winterberg M, Rajendran E, Baumeister S, Bietz S, Kirk K and Lingelbach K (2012) Chemical activation of a high-affinity glutamate transporter in human erythrocytes and its implications for malaria-parasite-induced glutamate uptake. *Blood* **119**:3604-3612.

MOL #81224

Footnotes

This research was supported by the Medicines for Malaria Venture (MMV) and the Intramural Research Program of the National Institutes of Health, National Institute of Allergy and Infectious Diseases.

Ajay D. Pillai and Wang Nguitragool contributed equally to this work.

Current addresses:

Ajay D. Pillai - Wellcome Trust/DBT India Alliance, Hyderabad, India

Wang Nguitragool - Department of Molecular Tropical Medicine and Genetics, Mahidol University, Bangkok, Thailand

Brian Lyko - Towson University, Towson, MD

Keithlee Dolinta - University of Texas MD Anderson Cancer Center, Houston, TX

Statement of Financial Interest: S.A.D. and A.D.P. are named inventors on provisional patent applications describing some of the PSAC inhibitors reported in this manuscript. M.M.B., S.T.N., N.P.P., and T.L.B. are employees and shareholders of Microbiotix, Inc., which has obtained a license to develop PSAC inhibitors as antimalarial drugs.

MOL #81224

Figure Legends

Fig. 1. Dose responses for parasite nutrient requirement and effect of ISPA-28. Normalized parasite growth rates over 72 h are shown in standard RPMI 1640-based media with indicated depletions of isoleucine, glutamine, or hypoxanthine (A, B, and C, respectively); all media were supplemented with 10% dialyzed human serum. Left and right panels show results for the Dd2 and HB3 parasite lines as indicated. In each panel, symbols represent mean \pm S.E.M. of 6-9 trials from up to 3 independent experiments; black and red symbols correspond to experiments without and with addition of 15 μ M ISPA-28, respectively. Solid lines represent best fit of data to sigmoidal growth curves. Note that ISPA-28 significantly increases Dd2 demand for isoleucine, but has no effect on that of HB3 parasites.

Fig. 2. ISPA-28 inhibits parasite growth via direct action on *clag3*-associated channels. (A) Parasite growth rates in PGIM as a function of [ISPA-28]. Notice that ISPA-28 inhibits growth of Dd2 (open triangles), but not of HB3 (filled circles). Solid lines represent best fits to a two-component exponential decay. (B) Mean \pm S.E.M. growth rates over 72 h in PGIM or pooled human serum (black and white bars, respectively), each normalized to 1 for matched cultures in RPMI 1640-based medium. (C) Mean \pm S.E.M. growth inhibition by 3 μ M ISPA-28 for indicated parental lines and progeny clones. Most progeny exhibit ISPA-28 sensitivity resembling one or the other parent. (D) Associated logarithm of odds (LOD) scores from a primary scan of QTL. The peak score maps to the *clag3* locus on parasite chromosome 3. Dashed line is the 0.05 significance threshold calculated from 1000 permutations. (E) ISPA-28 dose response for growth inhibition of HB3^{3rec} in PGIM. Solid lines are taken from panel A and represent the ISPA-28 sensitivities of HB3 and Dd2.

MOL #81224

Fig. 3. *In vitro* growth selection for *clag3* alleles associated with inhibitor-resistant channels.

(A) Schematic showing the two *clag3* genes of the 7C20 progeny clone. Active transcription of *clag3.1* is shown with a right angle arrow. (B) Strategy for purifying selections of *clag3.1* or *clag3.2* expression (blue and red cells, respectively). Osmotic lysis of 7C20-infected cells in sorbitol with ISPA-28 spares cells that express *clag3.1* (“transport selection”), while PGIM-based growth inhibition by ISPA-28 selects for *clag3.2* expression. (C) Mean \pm S.E.M. ISPA-28 dose responses for PSAC inhibition before (black circles) and after transport selection of the 7C20 line (blue) followed by PGIM growth selection (red). Solid lines represent the best fits to Eq.1. (D) Expression ratio for the two *clag3* alleles before and after these selections, determined by quantitative RT-PCR. High affinity ISPA-28 block is associated with *clag3.1* expression. Bars represent mean \pm S.E.M. of replicates from 2-4 separate trials each. (E) Mean \pm S.E.M. expression of the 5 *clag* genes before and after each selection.

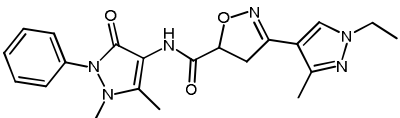
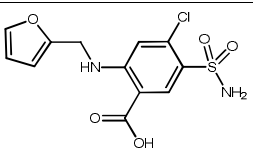
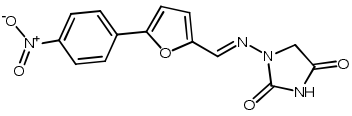
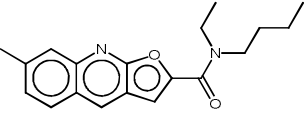
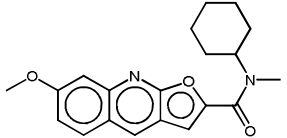
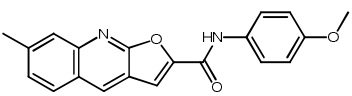
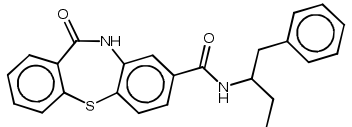
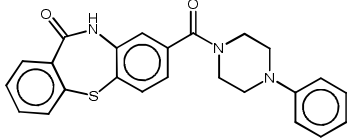
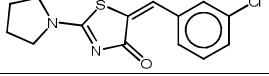
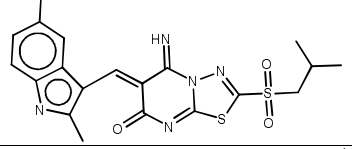
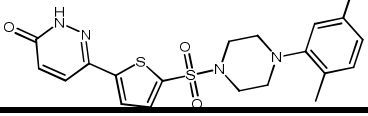
Fig. 4. Ectopic recombination of *clag3* genes in Dd2 parasites under selective pressure. (A) ISPA-28 dose response for PSAC inhibition in the Dd2-PGIM28 line (black circles, mean \pm S.E.M. of up to 5 measurements each). Solid lines are from Fig. 3C and reflect the dose responses for *clag3.1* and *clag3.2* expression in 7C20 (blue and red lines, respectively). (B) Ethidium-stained gels showing RT-PCR amplicons for expression of native *clag3* genes (“3.1” and “3.2”) or chimeric genes resulting from recombination (“3.1f-3.2r” and “3.2f-3.1r”). (C) PCR amplicons for native and chimeric *clag3* gene permutations from genomic DNA of indicated parasites. Dd2-PGIM28 carries and expresses a chimeric gene (“3.1f-3.2r”). (D) Southern blot showing three *clag3* copies in the Dd2-PGIM28 parasite, but only two in the original Dd2 line. DNA samples were digested with SphI or XbaI and detected with a *clag3* specific probe. The size of the additional band in Dd2-PGIM28 (16 kb, red arrow) is consistent

MOL #81224

with homologous recombination between the two *clag3* genes. (E) Schematic showing homologous recombination between the native *clag3* genes of Dd2 to produce three copies in Dd2-*PGIM28*. The site of recombination, indicated by a blue-to-red transition in the chimeric gene, was determined by DNA sequencing. The sites recognized by primers (used in panels B and C) and the probe used for Southern blotting (panel D) are indicated; vertical lines marked X and S represent XbaI and SphI restriction sites respectively, as used in the Southern blot. (F) Mean \pm S.E.M. expression of each *clag* gene in Dd2-*PGIM28* before and after transport-based selection for *clag3.1* using ISPA-28 (*PGIM-rev*). (G) Ratio quantifying relative expression of *clag3* and the chimeric gene, calculated from data in panel F and presented on a log scale. (H) PSAC inhibition by ISPA-28 in the *PGIM-rev* line. Solid lines are from Fig. 3C.

MOL #81224

Table 1. Broad spectrum PSAC inhibitors and antimalarial drugs that act at other sites.

Compound name	Structure	PSAC block $K_{0.5}$, nM	RPMI growth IC_{50} , μ M	PGIM growth IC_{50} , μ M	IC_{50} ratio
ISPA-28		Dd2: 56	> 40	0.66	> 60
		HB3: 43000	> 40	> 50	n/d
furosemide		2700	> 200	21	> 9.5
dantrolene		1200	42	3.8	18
cpd 1		87	23	0.27	114
cpd 3		33	15	0.17	86
cpd 9		6	18	0.23	270
cpd 2		84	4.7	0.41	15
TP-52		25	7.3	0.19	38
cpd 8		44	12.5	0.17	130
cpd 5		81	> 30	2.0	> 15
ISG-21		2.6	1.5	0.002	800
chloroquine		inactive	0.22	0.34	0.67
mefloquine		inactive	0.022	0.033	0.66
artemisinin		inactive	0.018	0.026	0.66

MOL #81224

Table 2. HeLa cell cytotoxicity and specificity index for parasite killing.

PSAC inhibitor	HeLa cell CC_{50} , μ M	Specificity (HeLa CC_{50} / parasite PGIM IC_{50})
cpd 1	30	110
cpd 9	> 100	> 430
cpd 2	> 100	> 240
TP-52	> 100	> 530
cpd 5	> 100	> 50
ISG-21	86	43,000

Figure 1

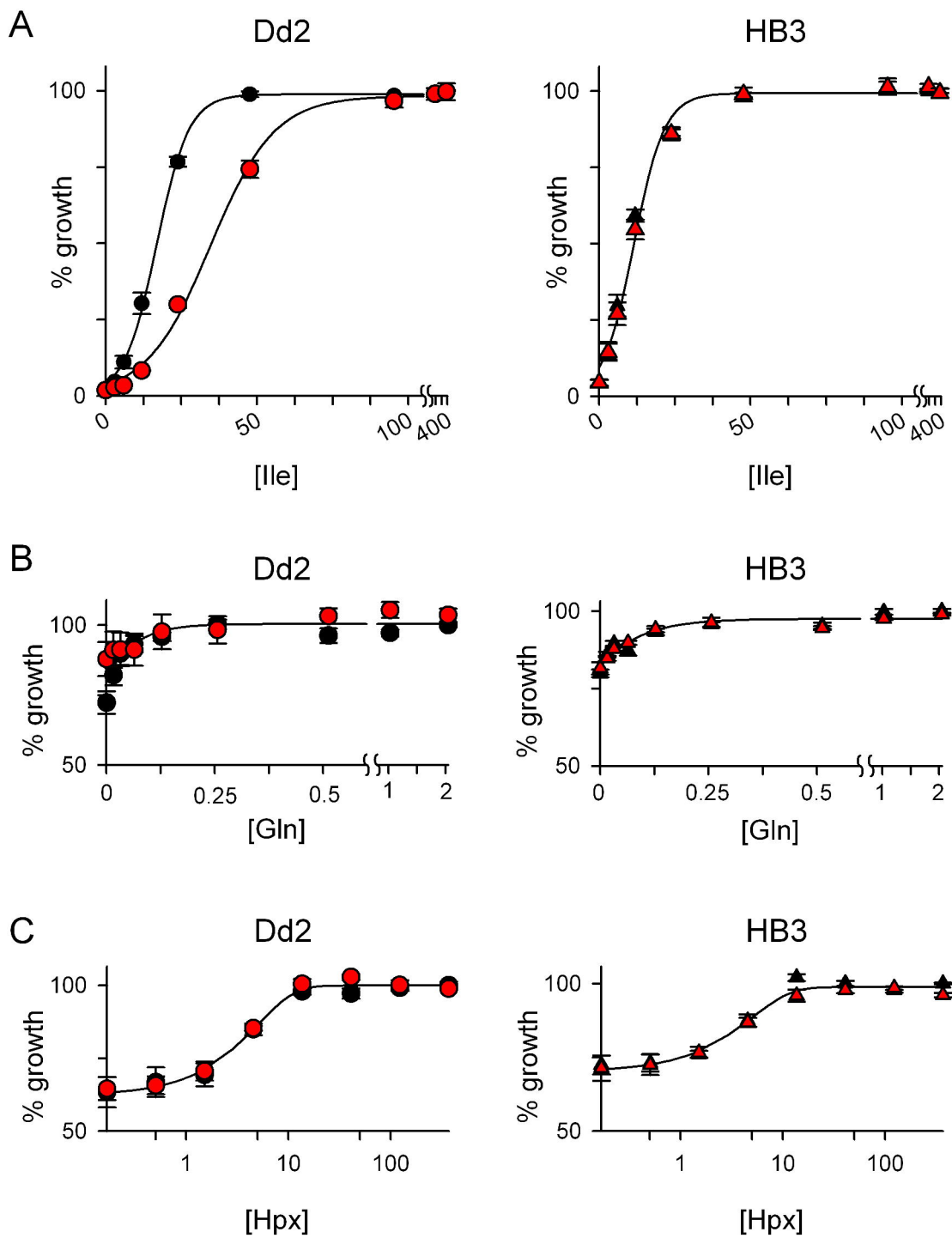


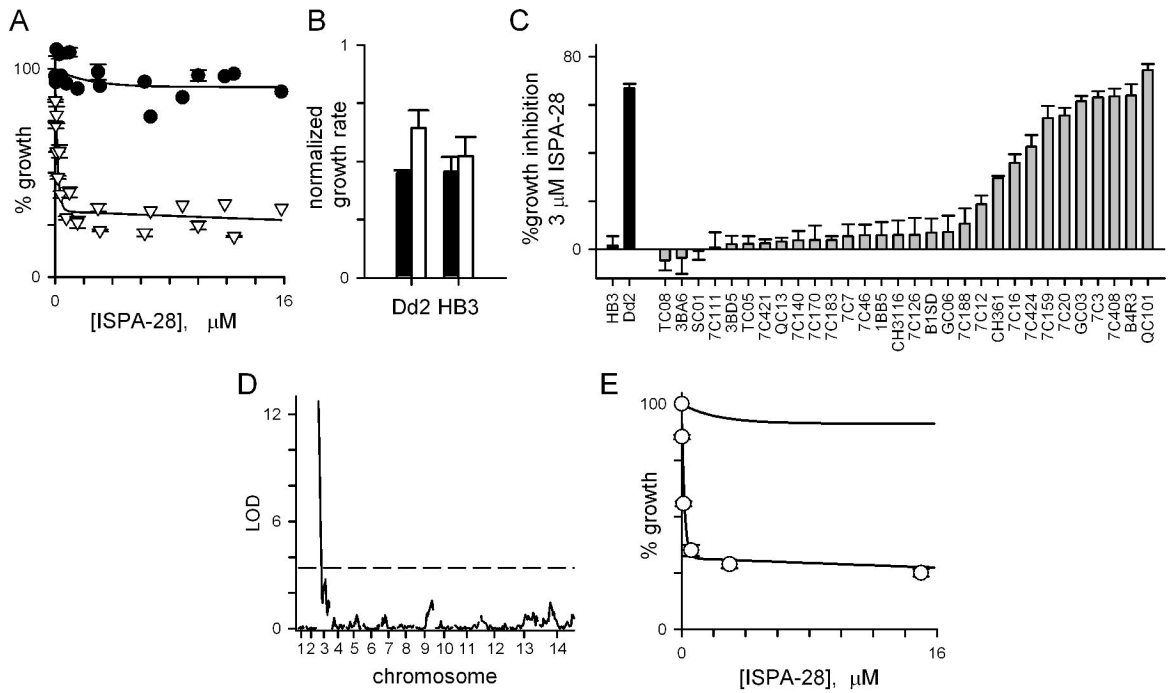
Figure 2

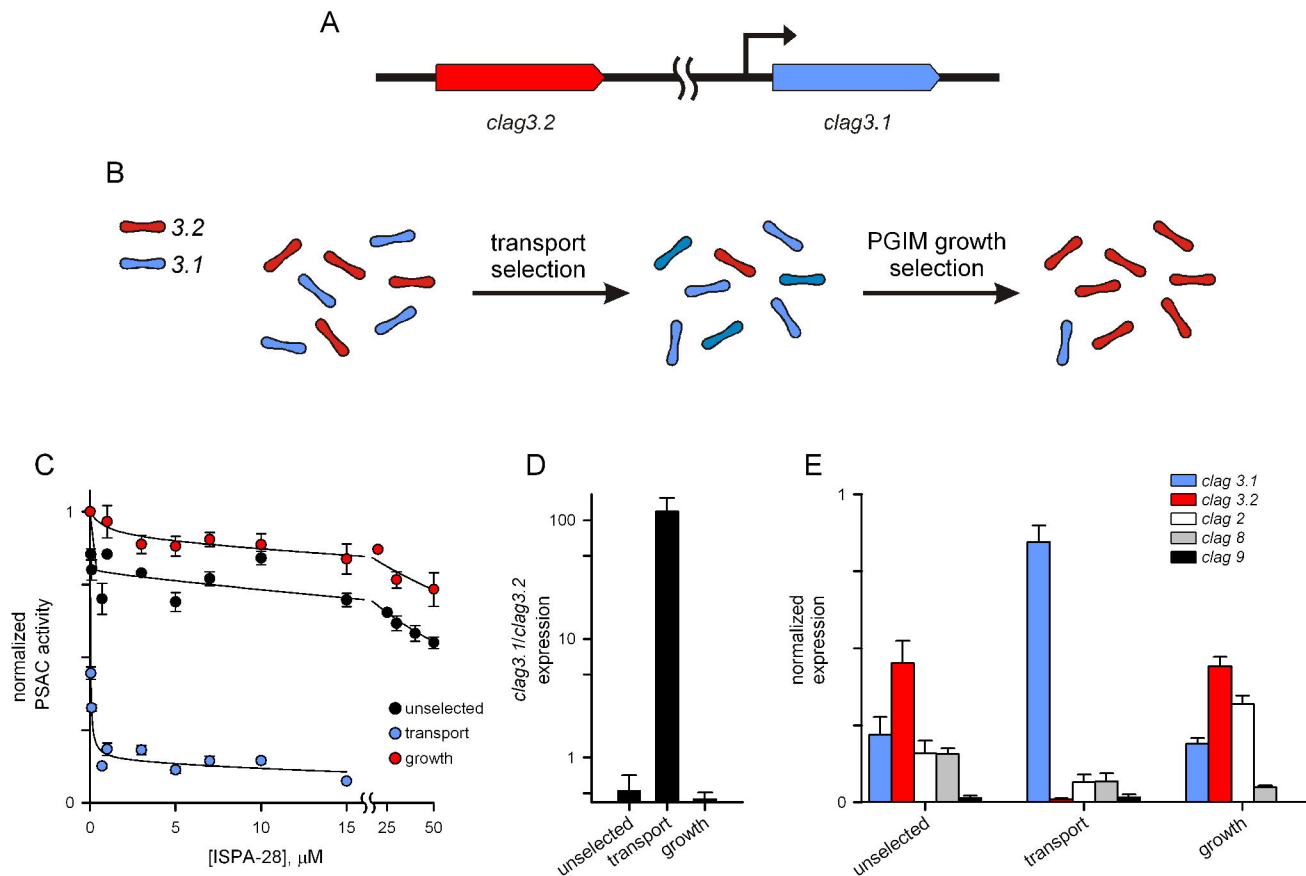
Figure 3

Figure 4

